BIOCHEMISTRY
including biophysical chemistry & molecular biology

Article

pubs.acs.org/biochemistry

Comparison of the Structural and Dynamic Effects of 5-Methylcytosine and 5-Chlorocytosine in a CpG Dinucleotide Sequence

Jacob A. Theruvathu,[†] Y. Whitney Yin,[†,‡] B. Montgomery Pettitt,[†,‡,§] and Lawrence C. Sowers*[,†,‡]

[†]Department of Pharmacology & Toxicology, The University of Texas Medical Branch, 3.330 Basic Science Building, 301 University Boulevard, Galveston, Texas 77555, United States

[‡]Sealy Center for Structural Biology & Molecular Biophysics, The University of Texas Medical Branch, 301 University Boulevard, Galveston, Texas 77555, United States

[§]Department of Biochemistry & Molecular Biology, The University of Texas Medical Branch, 301 University Boulevard, Galveston, Texas 77555, United States

Supporting Information

ABSTRACT: Inflammation-mediated reactive molecules can result in an array of oxidized and halogenated DNA-damage products, including 5-chlorocytosine (^{Cl}C). Previous studies have shown that ^{Cl}C can mimic 5-methylcytosine (^{m}C) and act as a fraudulent epigenetic signal, promoting the methylation of previously unmethylated DNA sequences. Although the 5-halouracils are good substrates for base-excision repair, no repair activity has yet been identified for ^{Cl}C. Because of the apparent biochemical similarities of ^{m}C and ^{Cl}C, we have investigated the effects of ^{m}C and ^{Cl}C substitution on oligonucleotide structure and dynamics. In this study, we have constructed oligonucleotide duplexes containing C, ^{Cl}C, and ^{m}C within a CpG dinucleotide. The thermal and thermodynamic stability of these duplexes were found to be experimentally indistinguishable. Crystallographic structures of duplex oligonucleotides containing ^{m}C or ^{Cl}C were determined to 1.2 and 1.9 Å resolution, respectively. Both duplexes are B-form and are superimposable on a previously determined structure of a cytosine-containing duplex with a rmsd of approximately 0.25 Å. NMR solution studies indicate that all duplexes containing cytosine or the cytosine analogues are normal B-form and that no structural perturbations are observed surrounding the site of each substitution. The magnitude of the base-stacking-induced upfield shifts for nonexchangeable base proton resonances are similar for each of the duplexes examined, indicating that neither ^{m}C nor ^{Cl}C significantly alter base-stacking interactions. The ^{Cl}C analogue is paired with G in an apparently normal geometry; however, the G-imino proton of the ^{Cl}C–G base pair resonates to higher field relative to ^{m}C–G or C–G, indicating a weaker imino hydrogen bond. Using selective ^{15}N-enrichment and isotope-edited NMR, we observe that the amino group of ^{Cl}C rotates at roughly half of the rate of the corresponding amino groups of the C–G and ^{m}C–G base pairs. The altered chemical shifts of hydrogen-bonding proton resonances for the ^{Cl}C–G base pair as well as the slower rotation of the ^{Cl}C amino group can be attributed to the electron-withdrawing inductive property of the 5-chloro substituent. The apparent similarity of duplexes containing ^{m}C and ^{Cl}C demonstrated here is in accord with results of previous biochemical studies and further suggests that ^{Cl}C is likely to be an unusually persistent form of DNA damage.

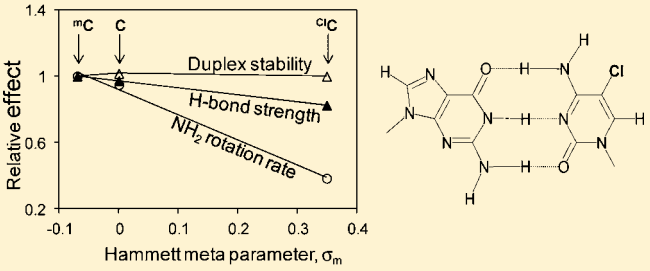

The development of cancer is driven by both genetic mutations and epigenetic dysregulation.[1−3] Although an extensive body of work has established mechanisms by which DNA damage can induce genetic mutations, substantially less is known about the relationship between DNA damage and epigenetic changes. In higher eukaryotes, the primary epigenetic mark in DNA is 5-methylcytosine (^{m}C), which modulates the transcriptional activity of key genes primarily by altering DNA–protein interactions.[4,5] In cancer cells, cytosine methylation patterns are corrupted, and frequently important tumor suppressor genes become silenced by aberrant promoter methylation.[6−8] Currently, there are few clear mechanisms to explain how aberrant promoter hypermethylation occurs.

Emerging evidence indicates that inflammation-mediated reactive molecules can modify DNA, creating an additional type of endogenous DNA damage.[9−11] Among the inflammation-mediated DNA adducts identified to date are the 5-halocytosines, 5-chlorocytosine (^{Cl}C) and 5-bromocytosine (^{Br}C), and both adducts have been identified in DNA from human tissues exposed to inflammation.[12−17] Although most types of DNA damage have been shown to interfere with enzymatic DNA methylation and with DNA-binding proteins

Received: July 22, 2013
Revised: October 17, 2013
Published: October 22, 2013

 © 2013 American Chemical Society dx.doi.org/10.1021/bi400980c | *Biochemistry* 2013, 52, 8590−8598

containing a methyl-binding domain, the 5-halocytosine analogues ^{Br}C and ^{Cl}C have been shown to mimic ^{m}C with respect to both DNA-binding proteins and methyltransferases.[18−21] Therefore, ^{Br}C and ^{Cl}C could act as fraudulent epigenetic signals, in part explaining how inflammation-mediated DNA damage could drive aberrant promoter methylation. Studies in eukaryotic cells have established that ^{Cl}C in DNA can result in heritable changes in promoter methylation.[22] Although ^{Br}C paired with G can be repaired slowly by both MBD4[18] and hTDG[23] glycosylases, no repair activities have yet been identified for ^{Cl}C and therefore ^{Cl}C could be a persistent form of DNA damage that would accumulate with increasing inflammation damage.

Previous studies have shown that the 5-halouracils can mimic thymine in DNA−protein interactions because the sizes of the 5-Cl, -Br, and -methyl substituents are similar.[24] However, because the inductive properties of the methyl substituent of thymine is electron-donating and the 5-halo substituents are electron-withdrawing, 5-halouracil analogues in DNA are rapidly repaired by multiple glycosylases.[25,26] We were therefore interested in understanding the impact of ^{Cl}C on oligonucleotide structure and dynamics to reveal how ^{Cl}C could serve as an excellent mimic for ^{m}C in several important biological interactions as well as avoid surveillance and detection by DNA-repair systems. In this study, we have constructed oligonucleotide duplexes containing cytosine, ^{m}C, and ^{Cl}C in the self-complementary Dickerson dodecamer sequence[27] within a CpG dinucleotide in one or both strands. We have studied these self-complementary duplexes in thermal-melting studies and X-ray crystallography as well as by ^{1}H NMR spectroscopy in solution to determine how ^{m}C and ^{Cl}C might differentially influence duplex structure and dynamics.

MATERIALS AND METHODS

Synthesis and Purification of Oligonucleotides. Oligonucleotides used in this study were synthesized by standard phosphoramidite solid-phase methods. To prepare oligonucleotides with 5-chlorocytosine, a phosphoramidite was prepared from O^4-ethyl-5-chloro-2′-deoxyuridine as previously described.[28] To prepare oligonucleotides containing ^{15}N-enriched 4-amino groups, phosphoramidites containing O^4-methyluracil (Glen Research, Sterling, VA), O^4-methylthymine (Glen Research), and O^4-ethyl-5-chlorouracil were coupled at the desired sequence position as shown in Figure 1. Oligonucleotides were then deprotected with ^{15}N-enriched aqueous ammonia (6 N, 98%, Cambridge Isotope Laboratories, Andover, MA) at room temperature for 36 h as previously describe for oligonucleotides containing 5-fluorocytosine.[29]

Oligonucleotides containing a dimethoxytrityl (DMT) group were purified by reverse-phase HPLC using a PRP column (Hamilton, Reno, NV), detritylated in 80% acetic acid at room temperature for 30 min, and then repurified by HPLC using a reverse-phase column. Following purification, oligonucleotides were characterized by MALDI-ToF-MS,[30] and the base composition of each was examined following formic acid hydrolysis and silylation by GC/MS (Supporting Information Figure S1).

Oligonucleotide UV Melting Studies. The melting temperature (T_m) and thermodynamic values of the self-complementary oligonucleotides were measured as previously described[31,32] using a Varian Bio 300 Cary UV−vis spectrophotometer (Palo Alto, CA). Oligonucleotides at selected total-strand concentrations from 2 to 60 μM were

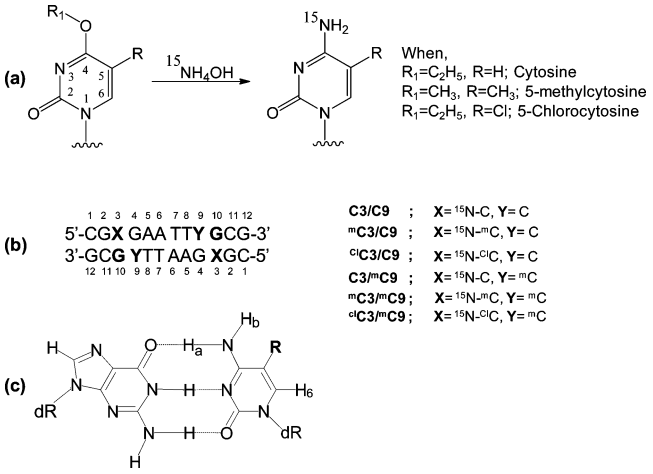

Figure 1. (a) Reaction scheme for the synthesis of ^{15}N-labeled oligonucleotide. (b) Dodecamer sequence and the oligonucleotides synthesized in this study. (c) Chemical structure of the G−C base pair. H_a is the Watson−Crick hydrogen and H_b is non-Watson−Crick hydrogen.

dissolved in a buffer containing 100 mM NaCl, 0.1 mM EDTA, and 10 mM sodium phosphate at pH 7. The T_m values are reported at 28 μM total-strand concentration.

Crystallography. Dodecamer self-complementary duplex oligos containing either ^{m}C or ^{Cl}C at position 3 ($^{m}C3/C9$ or $^{Cl}C3/C9$) were crystallized in solutions containing 50 mM HEPES, pH 7.0, 35−40% 2-methyl-2,4-pentanediol (MPD), 5−10 mM spermine, and 5−10 mM $MgCl_2$ at 17 °C. The crystals were directly frozen in liquid nitrogen. Diffraction data were collected at 100 K at the Advanced Photon Source, Argonne National Laboratory (Argonne, IL) using synchrotron radiation. Data were processed with the HKL3000 package (HKL Research, Inc., Charlottesville, VA), and structures were determined and refined using the PHENIX program.[33]

Nuclear Magnetic Resonance Spectroscopy (NMR). Solution NMR spectra were recorder with Bruker 500 or 300 MHz NMR systems (Billerica, MA). Proton NMR spectra were obtained in solution containing 10% D_2O/90% H_2O 100 mM NaCl, 10 mM sodium phosphate, and 0.2 mM EDTA at pH 7.0. To ensure duplex formation, oligonucleotides (200 A_{260} OD units, 2.5 mM) were heated at 86 °C for 2 min and slowly cooled to room temperature prior to acquisition of NMR spectra. Each spectrum was calibrated using DSS (4,4-dimetyl-4-silapentane-1-sulfonate) as an internal standard reference. Proton NMR spectra in aqueous solution were acquired with a water-suppression double-gradient echo WATERGATE W5 pulse program.[34] The temperature of the sample was controlled by a variable temperature monitor (Eurotherm, BVT 3000). Proton resonances were assigned from 2D NOE spectra.[35,36] The ^{15}N-edited proton NMR spectra were obtained using an HSQC pulse sequence.[37]

Rotational Dynamics. The ^{15}N-edited proton NMR experiments were used to study the dynamics of cytosine amino group (NH_2) rotation by observing the transfer of magnetization from one amino proton of the amino group to the other.[38,39] The resonance of each amino proton was selectively inverted by a rectangular soft pulse, and the effect of magnetization transfer from the inverted amino proton to the other was studied. The signal intensity of both amino protons was monitored as a function of the delay time after the

dx.doi.org/10.1021/bi400980c | Biochemistry 2013, 52, 8590−8598

Table 1. T_m and Thermodynamic Parameters for 5′-CGXGAATTYGCG-3′ in 10 mM Sodium Phosphate, 100 mM Sodium Chloride, and 0.1 mM EDTA at pH 7.0[a]

duplex	T_m (°C)	$\Delta H°$ (kcal mol^{-1})	$\Delta S°$ (cal mol^{-1} K^{-1})	$\Delta G°$ (25 °C) (kcal mol^{-1})
^{m}C3/C9	58.5 ± 0.5	−61.5 ± 5.8	−165 ± 18	−10.8 ± 0.5
^{m}C3/^{m}C9	58.7 ± 0.8	−61.9 ± 6.1	−166 ± 18	−10.8 ± 0.5
C3/C9	59.2 ± 0.1	−58.3 ± 9.0	−154 ± 27	−10.7 ± 0.8
C3/^{m}C9	59.9 ± 0.8	−59.3 ± 8.9	−157 ± 27	−10.9 ± 0.8
^{Cl}C3/C9	58.2 ± 0.2	−62.4 ± 10	−168 ± 31	−10.7 ± 0.7
^{Cl}C3/^{m}C9	58.9 ± 0.7	−60.5 ± 11	−162 ± 33	−10.6 ± 0.7

[a] T_m values are at 28 μM total-strand concentration.

inversion pulse, ranging from 5 μs to 4 s. In the experiments described here, the magnetization of a particular amino proton at a particular time will be according to eq 1

$$M(t) = M^0 + C^*\exp(\lambda_1 t) + F^*\exp(\lambda_2 t) \quad (1)$$

where λ_1 and λ_2 are

$$\lambda_1 = -(R_{1A} + R_{1B})/2 - \sigma \quad (2)$$

and

$$\lambda_2 = -(R_{1A} + R_{1B})/2 - 2k_r + \sigma \quad (3)$$

M^0 is the equilibrium magnetization and C and F are constant coefficients depending on the relaxation rates of the two protons. R_{1A} and R_{1B} are the longitudinal relaxation rates, k_r is the rate of rotation, and σ is the cross relaxation rate. Values for λ_1 and λ_2 are obtained from the nonlinear fit of the plot of the intensity of the amino-proton resonance versus delay time using eq 1. Rotation rates are obtained from λ_1 and λ_2 using eqs 2 and 3. The cross relaxation rate (σ) is determined from the initial NOE buildup rate at lower mixing times (5−40 ms).

Quantum Mechanical Studies of 5-Chlorocytosine. Quantum mechanical calculations[40,41] were performed with the Gaussian 03 program (Gaussian, Inc., Wallingford, CT) on a Pentium pro quad processor. Density functional theory (DFT) calculations were performed with the 6-31G basis set (B3LYP) within the Gaussian software. The template structure of 2′-deoxycytidine (dC) was used as the initial structure. The template structure of dC was edited to create the corresponding 5-methyl- and 5-chloro-2′-deoxynucleosides. Bond lengths for each molecule were obtained from the energy-minimized structures.

RESULTS

The synthetic approach presented here yields oligonucleotides containing selected ^{15}N-enriched cytosine amino groups. The ^{15}N-amino groups are introduced during the final deprotection of the oligonucleotides. Therefore, this is an efficient method for inserting one or more labels site-specifically in either cytosine or cytosine analogues (Figure 1). Previously, ^{15}N-enriched cytosine amino groups have been introduced into oligonucleotides by synthesis of the ^{15}N-enriched phosphoramidite or by introduction of a 4-triazole phosphoramidite.[42−44] As precursors for the introduction of the 5-fluorocytosine or 5-chlorocytosine, we find the O^4-ethyl analogues to be suitably stable during phosphoramidite and oligonucleotide synthesis and to be quantitatively displaced by ammonia during oligonucleotide deprotection with minimal hydrolysis to the corresponding uracil analogues. Base and isotopic composition of the oligonucleotides listed in Table 1 were verified by both MALDI-ToF-MS and GC/MS (Supporting Information Figure S1).

As a first approach to identify potential perturbations in oligonucleotide structure and dynamics, the thermal and thermodynamic properties of a series of oligonucleotides containing C, ^{Cl}C, or ^{m}C were investigated by examining duplex dissociation as a function of temperature (Figure 2).

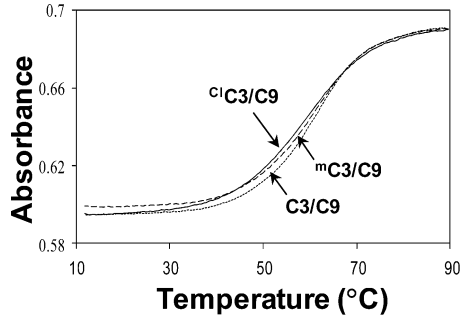

Figure 2. Normalized melting profiles at 260 nm of 28 μM oligonucleotides in presence of 10 mM sodium phosphate, 100 mM sodium chloride, and 0.1 mM EDTA at pH 7.0.

Thermodynamic parameters were obtained by fitting the experimental melting curves or from a plot of $1/T_m$ versus ln Ct obtained at different oligonucleotide concentrations (Ct) as described previously[31,32] (Supporting Information Figure S2). The experimental values obtained in this study for the oligonucleotides shown in Figure 1 are listed in Table 1. The experimental T_m values obtained in this study are close to the value of 59 °C predicted for the cytosine-containing duplex on the basis of the nearest-neighbor model of SantaLucia et al.[45] In thermal melting studies, T_m values can be measured reproducibly to within 0.5 °C. In the sequences studied here containing one modified cytosine analogue and either cytosine or ^{m}C in the opposing strand of the CpG dinucleotide, observed melting temperatures for the ^{Cl}C and ^{m}C duplexes are experimentally indistinguishable (Figure 2). Therefore, in the sequences studied here, both ^{m}C and ^{Cl}C have no measurable impact on duplex thermal stability.

To determine the comparative impact of C, ^{m}C, and ^{Cl}C on duplex structure, oligonucleotide duplexes were studied by X-ray crystallography and by NMR spectroscopy in aqueous solution. The crystal structure of a duplex containing ^{m}C was determined to 1.2 Å resolution and refined to an R-factor of 0.249 (R_{free} = 0.278) by the molecular-replacement method using an unmodified Dickerson−Drew dodecamer (PDB ID: 1FQ2). The structure of the ^{Cl}C-containing duplex was determined using the same method to 1.9 Å and refined to an R-factor of 0.195 (R_{free} = 0.262) (Supporting Information

dx.doi.org/10.1021/bi400980c | Biochemistry 2013, 52, 8590−8598

Table S1). The ^{m}C and ^{Cl}C structures closely resemble each other, with a rmsd of 0.25 Å. Both duplexes adopt a B-form DNA configuration, with rmsd of 0.22 and 0.23 Å relative to the Dickerson–Drew duplex containing cytosine (Figure 3).

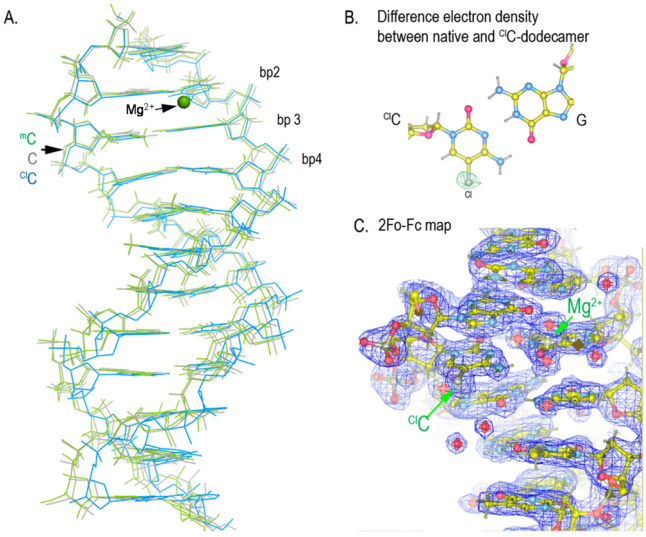

Figure 3. Structure of the Dickerson–Drew dodecamer with a modified base at position 3. (A) Superposition of the ^{m}C (green)- and ^{Cl}C (blue)-containing duplex with native C dodecamer (gray). (B) Difference map between the ^{Cl}C and C dodecamers ($F_o^{ClC} - F_c^{C}$, Φ^{ClC}) revealing electron density around Cl on ^{Cl}C at position 3. (C) Electron density ($2F_o - F_c$) for the ^{Cl}C-containing dodecamer. F_o is the observed electron density map, and F_c is the calculated electron density map. The structure factors and coordinates of the ^{Cl}C- and ^{m}C-containing dodecamers are deposited at the Protein Data Bank under accession numbers 4MGW and 4MKW, respectively.

A more detailed comparative structural analysis was performed on each duplex examined here using the program CURVES+[46] and the corresponding crystallographic PDB files as input. The CURVES+ program can reveal more subtle differences in the orientation of the base-pair axis (BP-axis), base rotation, and translation as well as other helical parameters. Data obtained with the CURVES+ program is tabulated in Supporting Information Table S2, with values for each modified base pair as well as average values for all base pairs in each duplex. Differences among the cytosine, ^{Cl}C, and ^{m}C duplexes are modest, and the values for the ^{Cl}C and ^{m}C duplexes are usually more similar to one another than to that for the cytosine-containing oligonucleotide.

NMR studies in aqueous solution were performed to examine potential dynamic influences of each substitution. The aromatic base and H1′ sugar residues for each duplex were observed and assigned by standard 2D NMR methods (Supporting Information Figure S3). Chemical shifts are tabulated in Supporting Information Tables S3 and S4. The observed NOE connectivities are consistent with a predominantly B-form helix in which all of the bases are intrahelical (Supporting Information Figure S4). Significant differences are noted for the chemical shifts of the H6 protons for C, ^{m}C, and ^{Cl}C in each of the duplexes examined. To determine the effect of the 5-substituent on the chemical shift of the H6 proton, NMR spectra were also recorded for the corresponding free 2′-deoxynucleosides in D_2O (Supporting Information Table S5).

The proton NMR spectrum of the exchangeable-proton region for each duplex at 300 K showed five imino proton resonances for these symmetric 12-base duplexes (Figure 4).

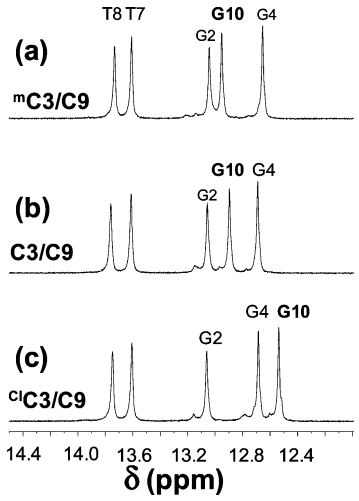

Figure 4. ^{1}H NMR spectra in the imino region of the [4-^{15}N] labeled (X3 position, Figure 1) oligonucleotides (a) ^{m}C3/C9, (b) C3/C9, and (c) ^{Cl}C3/C9 in the presence of 10% D_2O, 100 mM NaCl, 10 mM sodium phosphate, and 0.2 mM EDTA at pH 7 and 300 K.

The imino protons of the terminal base pairs are exchange-broadened under these conditions and are not observable. However, the terminal imino protons are observed at lower temperature (Supporting Information Figure S5). For the three duplexes containing C, ^{m}C, or ^{Cl}C at position 3, the imino region is essentially the same with one exception. The chemical shift of the imino proton of G10, paired with the C or substituted C at position 3, is different in each spectrum, ranging from 12.95 ppm when paired with ^{m}C to 12.54 ppm when paired with ^{Cl}C. A similar trend was observed in duplexes containing ^{m}C in the opposing strand (Supporting Information Table S6).

The amino protons of the cytosine residues are observed in a spectrally crowded region between 6 and 9.5 ppm (Figure 5). The amino proton hydrogen-bonded to the G residue is shifted downfield relative to the non-hydrogen-bonded amino proton. To directly observe the amino protons of the cytosine residue at oligonucleotide position 3, the nitrogen of the amino groups was ^{15}N-enriched. Selective enrichment permits direct observation of the *J*-coupled amino protons, as shown in Figure 5a. The amino resonances observed in ^{15}N-decoupled spectra are shown in Figure 5b–d. The observed imino and amino proton resonances indicate that G pairs with ^{m}C and ^{Cl}C in a hydrogen-bonding pattern similar to the Watson–Crick C–G base pair.

To examine the dynamics of the target cytosine residue at position 3, the rotation rate of the amino group was measured by the saturation-transfer method described in the Materials and Methods and is shown in Supporting Information Figures S6 and S7. The rotational rates of C, ^{m}C, and ^{Cl}C in the corresponding oligonucleotides are 32.9, 33.4, and 12.7 s^{-1}, respectively (Table 2). The placement of a ^{m}C residue in the opposing strand had minimal impact on the amino group rotation rate (Table 2), and in both sequence contexts, the amino group of the ^{Cl}C residue rotates at approximately half of the rate of the corresponding ^{m}C residue. The line width of the G-imino proton of the X3–G10 base pair was also measured as

dx.doi.org/10.1021/bi400980c | *Biochemistry* 2013, 52, 8590–8598

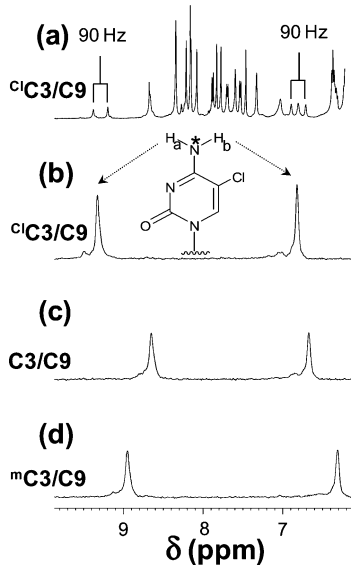

Figure 5. (a) ^{1}H NMR spectrum (unedited) of the [4-^{15}N] ^{Cl}C3/C9 oligo. (b–d) ^{15}N-edited proton spectrum of ^{15}N-labeled oligonucleotides in the presence of 10% D_2O, 100 mM NaCl, 10 mM sodium phosphate, and 0.2 mM EDTA at pH 7 and 300 K. The ^{15}N label is indicated in the structure by the asterisk.

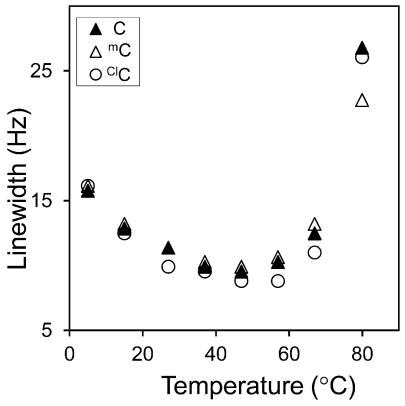

Figure 6. Temperature-dependent line-width studies of G10 imino protons of C3/C9, ^{m}C3/C9, and ^{Cl}C3/C9 oligonucleotides in the presence of 10% D_2O, 100 mM NaCl, 10 mM sodium phosphate, and 0.2 mM EDTA at pH 7 and 300 K.

a function of temperature. For the three duplexes examined here, the temperature dependence of the G-imino proton resonance line width overlapped substantially, as shown in Figure 6.

DISCUSSION

Substitution with ^{Cl}C Does Not Alter Duplex Stability as Measured in Thermal-Melting Studies. In this study, a total of six symmetric oligonucleotides forming six duplexes were studied. Each oligonucleotide contained ^{m}C, C, or ^{Cl}C at position X3 (Figure 1b). Three of the duplexes contained C at position Y9 (Figure 1b), whereas three contained ^{m}C at position Y9. In eukaryotic DNA, ^{m}C is usually found in symmetrically methylated ^{m}CpG dinucleotides; however, ^{m}C can also be found in hemimethylated CpG dinucleotides following DNA replication prior to maintenance methylation.[20] Oligonucleotide melting temperatures are measured by observing optical absorbance as a function of temperature (Figure 2). Thermodynamic parameters are extracted from the melting studies either by curve-fitting or by measuring melting temperature as a function of oligonucleotide concentration,[31,32] and the differences obtained with each method were at or below experimental error. The thermal and thermodynamic parameters for duplex dissociation are given in Table 1. In the duplexes examined here, changes in duplex melting temperature resulting from the replacement of C by ^{m}C or ^{Cl}C were at or below the experimental error. Similarly, thermodynamic differences were at or below experimental error. Therefore, the replacement of ^{m}C by ^{Cl}C has little or no observable impact on the thermal or thermodynamic stability of an oligonucleotide duplex, at least within the sequence examined here. Previous studies have shown that cytosine methylation generally increases oligonucleotide melting temperatures; however, the increase is modest and sequence-dependent.[47,48]

Crystal Structures of the C, ^{m}C, and ^{Cl}C Duplexes Are Superimposable. The duplex structures of the ^{Cl}C3/C9 and ^{m}C3/C9 oligonucleotides were examined by crystallography and compared with the native Dickerson dodecamer (C3/C9). All of the duplexes form typical B-form geometry. The ^{Cl}C or ^{m}C substitution in position 3 of the sequence had negligible effect upon the structures (Figure 3). Consistent with our findings, previous studies have shown that the 5-bromocytosine within the same sequence context is also B-form and is isomorphous to the native structure.[27] Oligonucleotides containing 5-methylcytosine or 5-bromocytosine have been shown to promote alternative A or Z forms depending on the sequence context;[49] however, these alternative forms require unusual DNA sequences.

Examination of Nonexchangeable Protons Reveals the Similarity of the ^{Cl}C and ^{m}C Duplexes. Upon duplex

Table 2. Amino Proton Chemical Shifts, Rate of Rotation of Amino Protons, and Line Widths of the Amino Resonances of the Third Base of the Oligonucleotide (Figure 1) at 300 K and pH 7[a]

		chemical shifts of X3 amino protons in oligos					line width (Hz)	
duplex	k_r (sec^{-1})	NH_2 H_a	NH_2 H_b	$\Delta\delta$ (H_a – H_b)	$\Delta\delta$a	$\Delta\delta$b	H_a	H_b
^{m}C3/C9	33.4	8.95	6.31	2.64	2.06	−0.58	31.9	26.8
^{m}C3/^{m}C9	36.9	9.00	6.23	2.77	2.11	−0.66	34.1	28.6
C3/C9	32.9	8.65	6.68	1.97	1.89	−0.56	33.0	25.7
C3/^{m}C9	33.8	8.68	6.59	2.09	1.92	−0.65	33.7	28.6
^{Cl}C3/C9	12.7	9.31	6.81	2.50	1.95	−0.43	26.8	21.6
^{Cl}C3/^{m}C9	14.1	9.38	6.74	2.64	2.02	−0.50	25.3	22.4

[a]Rate of rotation (k_r) was determined by ^{15}N-edited magnetization-transfer experiments, and line widths (half height width) were determined using ^{15}N-edited experiments. $\Delta\delta$a = H_a – monomer H_a and $\Delta\delta$b = H_b – monomer H_b.

dx.doi.org/10.1021/bi400980c | Biochemistry 2013, 52, 8590–8598

formation, the solution ^{1}H NMR chemical shifts of nonexchangeable protons are observed to move upfield relative to monomer chemical shifts because of base−base-stacking interactions. In the duplex, the nonexchangeable resonances can be assigned by sequential NOE connectivities,[35,36] as shown and tabulated in the Supporting Information (Tables S3 and S4). The observed nonexchangeable base proton−H1′ connectivities indicate that all duplexes studied here are predominantly B-form and that all bases are intrahelical.

The magnitudes of the upfield shifts of the nonexchangeable resonances are proportional to the degree of base-stacking interactions and are sensitive indicators of base geometry within the duplex. With one exception, the chemical shifts of the nonexchangeable aromatic proton resonances are invariant among the duplexes containing ^{m}C, C, and ^{Cl}C at position X3 when Y9 is C or ^{m}C (Supporting Information Figure S3). The single exception in each case is the chemical shift of the H6 proton of the ^{m}C, C, or ^{Cl}C residue at position X3, where these resonances are observed at 7.04, 7.25, and 7.54−7.55 ppm, respectively, when Y9 is either C or ^{m}C. The observed chemical shift of the H6 resonance in a duplex is dependent upon both the intrinsic chemical shift of the proton resonance and the base-stacking change resulting from duplex formation. In pyrimidine analogues, a 5-substituent can significantly alter the chemical shift of H6, with electron-donating substituents such as CH_3 moving the chemical shift to higher field and electron-withdrawing substituents shifting in the opposing direction. The chemical shifts of the H6 proton for the corresponding 2′-deoxynucleosides in water at 300 K are 7.64, 7.81, and 8.11 ppm for ^{m}dC, dC, and ^{Cl}dC, respectively. The stacking-induced shifts in the sequence examined here are observed to be 0.60, 0.56, and 0.56 for ^{m}C, C, and ^{Cl}C, respectively, and therefore the observed H6 chemical-shift differences among the duplexes examined are dominated by the 5-substituent effect on the intrinsic chemical shift of the corresponding H6 proton. The similarity in the base-stacking induced change in the H6 chemical shift across the duplexes examined here is consistent with a negligible effect of ^{Cl}C substitution on duplex stability or conformation.

Examination of Exchangeable Protons Resonances Reveals Differences between the Duplexes. Upon duplex formation, the resonances of exchangeable amino and imino protons become narrower and shift downfield because of the formation of hydrogen bonds with bases in the complementary strand. The imino-proton regions of duplexes containing ^{m}C, C, and ^{Cl}C with C at position Y9 are shown in Figure 4. With the exception of the chemical shift of the G10 resonance of the X3−G10 base pair, the spectra are largely indistinguishable. The G10 imino proton from the ^{Cl}C−G base pair is high field of the other G imino protons but is well within the range expected for a normal Watson−Crick base pair.

A substituent in the 5-position of the cytosine ring can influence the basicity of the N^3 position, which is the hydrogen-bond acceptor for the G10 imino proton. The pK_a of the N^3 position of dC is 4.2, and an electron-donating CH_3 substituent in the 5-position increases the pK_a to 4.3.[29] In contrast, an electron-withdrawing Cl substituent decreases the pK_a of ^{Cl}dC to 2.7.[29] In Figure 7a, the G10 chemical shift is plotted versus the pK_a of the paired cytosine or cytosine analogue, and a linear relationship is observed. The presence of a cytosine 5-substituent has an observable effect upon the G−C imino hydrogen bond, which is proportional to the substituent effect on the corresponding N^3 pK_a value.

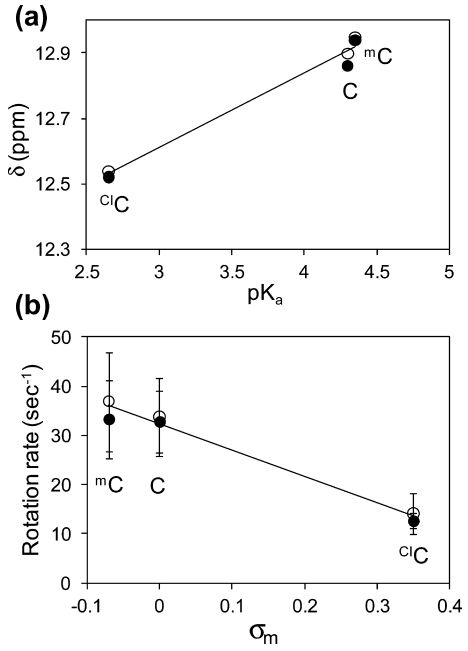

Figure 7. (a) Proton chemical shifts of the G imino protons of the X3−G10 base pair of the oligonucleotide versus the pK_a of the corresponding nucleoside at pH 7, where X3 is ^{m}C, C, or ^{Cl}C. (b) Amino group rotation rate as a function of the Hammett σ_m parameter of the 5-substituent. Closed circles are for the X3/C9 oligo, whereas open circles are for the X3/^{m}C9 oligo.

The dynamics of the base pair formed between X3 and G10 can also be investigated by examining the line width of the G10 imino resonance as a function of temperature. The G10 imino proton line widths for duplexes containing ^{m}C, C, and ^{Cl}C are shown in Figure 6. As the temperature is increased from 5 °C, the line width for each duplex decreases and then increases because of enhanced base-pair opening and proton exchange with solvent. However, the line widths for the three duplexes are very similar and appear to converge around physiological temperature. These data suggest that although the presence of ^{Cl}C decreases the strength of the imino hydrogen bond with G10 the ^{Cl}C−G base pair is held intact by base-stacking interactions and does not open with greater frequency than the corresponding base pairs with C or ^{m}C, consistent with the thermodynamic results presented above.

The strength of the hydrogen bond can also be estimated by the downfield shift of the imino proton within the oligonucleotide relative to its monomer value. The intrinsic chemical shift of the imino proton of the 2′-deoxyguanosine nucleoside is 10.59 ppm (in DMSO), whereas the chemical shifts of guanine imino protons (G10) in C−G, ^{m}C−G, and ^{Cl}C−G base pairs are 12.90, 12.95, and 12.54 ppm, respectively, for the C3/C9, ^{m}C3/C9, ^{Cl}C3/C9 oligonucleotides. The difference in chemical shift between the oligo and corresponding nucleoside are 2.31, 2.36, and 1.95 ppm for the C3/C9, ^{m}C3/C9, and ^{Cl}C3/C9 oligonucleotides, which indicates that the ^{m}C3−G10 base pair has the strongest hydrogen bond, whereas the ^{Cl}C3−G10 base pair has the weakest hydrogen bond. Similar relative magnitudes of base-pairing-induced shifts were observed for oligonucleotides in which ^{m}C was placed in the opposing strand.

The dynamics of the base pairs formed between G10 and ^{m}C, C, and ^{Cl}C can also be examined by observation of the amino

dx.doi.org/10.1021/bi400980c | Biochemistry 2013, 52, 8590−8598

protons of the paired cytosine or cytosine analogue. The amino protons of cytosine analogues rotate at a relatively slow rate on the NMR time scale and can be observed as separate resonances. With monomeric 2′-deoxycytidine (dC) in solution, the hydrogen-bonding H_a or Watson−Crick (WC) proton is exchange-broadened and shifted to high field of the non-hydrogen-bonding non-Watson Crick (nWC) proton, H_b (Figure 1c). With ^{m}dC, both amino protons are coincident; however, with ^{Cl}dC, the WC proton H_a is shifted to low field of the nWC proton H_b (Supporting Information Table S5). Within the dC series, a 5-substituent has a much greater effect upon the chemical shift of the nWC proton. When comparing the line width of the H_a and H_b protons of dC and ^{Cl}dC at 5 °C, the H_a proton is broader than H_b in all cases. The line widths of the H_a protons for dC and ^{Cl}dC are 33.4 versus 29.2 Hz, respectively; however, the line width of ^{Cl}dC H_b is only 13.1 Hz, whereas H_b for dC is 23.0 Hz. The line widths for the ^{m}dC (monomer) amino protons could not be determined because of resonance overlap. The observed line width is a function of both chemical exchange with solvent and rotational line broadening. The data reported here suggest that in the monomers, dC and ^{Cl}dC, the rates of chemical exchange are similar (H_a). However, the narrower line width of H_b for ^{Cl}dC indicates that the amino group is rotating more slowly relative to dC.

The amino resonances of ^{15}N-isotope-enriched ^{m}C, C, and ^{Cl}C within duplex oligonucleotides were edited from a crowded spectral region and assigned as shown in Figure 5. In each duplex, the H_a proton moves considerably downfield because of hydrogen-bond formation with the O^6 position of G10 and becomes substantially narrower, whereas the H_b proton moves slightly upfield because of base-stacking interactions. The magnitude of the hydrogen-bonding-induced change in H_a chemical shift for ^{m}C, C, and ^{Cl}C are 2.06, 1.89, and 1.95 ppm, whereas the corresponding changes for the ^{m}C9 oligos are 2.11, 1.92, and 2.02 ppm. These data confirm the formation of a base pair between ^{Cl}C and G10 that approximates Watson−Crick geometry.

The rate of rotation of an amino group can be studied by using magnetization transfer as demonstrated previously by Russu and co-workers,[38,39] and values obtained with these methods are given in Table 2. The rotation rate of the ^{m}C amino group (X3 = ^{m}C) is approximately 33 s^{-1} when Y9 is C and 37 s^{-1} when Y9 is ^{m}C. In the C-containing duplex (X3 = C), the amino group rotation rate is approximately 33 s^{-1} when Y9 is either C or ^{m}C. In contrast, the apparent rate of the ^{Cl}C amino group (X3 = ^{Cl}C) is 12.7 s^{-1} (Y9 = C) but increases to 14.1 s^{-1} when ^{m}C is in the opposing strand (Y9 = ^{m}C). The temperature-dependent line-width analysis shows that the labeled amino resonance of the ^{Cl}C3/C9 oligonucleotide broadens slower than those in the C3/C9 or ^{m}C3/C9 oligonucleotides, which indicates that the ^{Cl}C amino group rotates more slowly (Supporting Information Figure S8).

The reduced rate of rotation of the amino group of ^{Cl}C relative to C or ^{m}C could be attributed to a reduced rate of base-pair opening or to a slower intrinsic rotation rate resulting from the 5-chloro substituent. A previous study has shown that the C^4−N^4 bond of cytosine and its analogues have considerable double-bond character,[40] consistent with its slow amino group rotation rate relative to adenine and guanine analogues. We investigated the geometry of the ^{m}dC, dC, and ^{Cl}dC monomers through DFT calculations performed with the 6-31G basis set (B3LYP). The C^4−N^4 bond lengths of ^{m}dC, dC, ^{Cl}dC were found to be 1.363, 1.364, and 1.355 Å, respectively. The reduced C^4−N^4 bond length of ^{Cl}dC is consistent with more double-bond character and would result in a reduced rate of amino group rotation, as observed in studies with the monomers discussed above.

Consistent with the computational results discussed above, the rate of rotation of the cytosine amino group in the duplexes examined here is related to the electronic-inductive property of the 5-substituent. A linear relationship (Figure 7b) is obtained when the amino group rotation rate is plotted versus the Hammett parameter (σ_m) for ^{m}C, C, and ^{Cl}C. The Hammett parameters for the selected substituents are obtained from Hansch et al.[50] The methyl group of ^{m}C is electron-donating, whereas the Cl substituent of ^{Cl}C is electron-withdrawing. Therefore, the slower rotation rate of the ^{Cl}C amino group in the duplex can be attributed primarily to the electronic-inductive effect of the 5-Cl substituent.

Summary and Conclusions. A series of oligonucleotide duplexes were constructed containing ^{m}C, C, and ^{Cl}C with either C or ^{m}C in the opposing strand within a CpG dinucleotide. Optical melting studies indicate that the replacement of C or ^{m}C with ^{Cl}C does not alter observably duplex thermal or thermodynamic stability. Results of crystallographic and ^{1}H NMR studies establish that the overall geometries of the ^{Cl}C-containing duplexes are normal, B-form, and that the base pair formed between ^{Cl}C and G approximates Watson−Crick geometry. A correlation is observed between the chemical shift of the imino proton of the G residue and the pK_a of the N^3 position of the paired cytosine analogue for the series ^{m}C, C, and ^{Cl}C, suggesting that the electron-withdrawing 5-chloro substituent, which reduces the pK_a of the N^3 position, proportionately decreases the strength of the G−^{Cl}C imino hydrogen bond. Despite an apparently reduced imino hydrogen-bond strength, the G imino proton of the G−^{Cl}C base pair is not unusually broadened with increasing temperature, suggesting that the local base-stacking, which is unchanged by ^{Cl}C substitution, is sufficient to maintain the base pair in a predominantly closed state. The H_a amino proton of ^{Cl}C forms a hydrogen bond with the O^6 position of the paired G residue, and the ^{Cl}C amino group rotates at approximately half of the rate of the C or ^{m}C amino groups. The reduced rate of amino group rotation is attributed to the 5-chloro substituent increasing the double-bond character of the C^4−N^4 bond of ^{Cl}C as opposed to slowing the rate of base-pair opening. These results are in accord with previous biochemical findings that ^{Cl}C is a very good mimic for ^{m}C and that it can act as a fraudulent epigenetic signal. Prior studies on DNA-damage recognition have shown that glycosylases of the base-excision-repair pathway can exploit structural and thermodynamic perturbations of damaged base pairs in distinguishing modified and normal bases in DNA.[26,51,52] The apparent structural and dynamic similarities between ^{Cl}C and ^{m}C oligonucleotides shown here are in accord with the reported inability of glycosylases to recognize and remove ^{Cl}C from DNA. Therefore, the formation of ^{Cl}C in DNA poses a significant challenge for base-excision repair, and ^{Cl}C is likely to accumulate in DNA over time as a function of inflammation exposure and might, in part, explain the established relationship between inflammation and cancer development.[53,54]

■ ASSOCIATED CONTENT

Supporting Information

Crystallographic data collection and refinement statistics of the oligonucleotide ^{m}C3/C9 and ^{Cl}C3/C9; helicoid analyses of Dickerson−Drew dodecamers containing ^{m}C or ^{Cl}C at position 3 (^{m}C3/C9 and ^{Cl}C3/C9); chemical shifts of the selected nonexchangeable protons of the oligonucleotides; chemical shifts and line width of amino protons of the nucleosides in 10% D_2O at 5 °C; chemical shift of imino protons of the oligonucleotides; characterization of the ^{Cl}C3/C9 oligonucleotide by GC−MS and MALDI ToF; $1/T_m$ versus ln(Ct) plot for the $^{m}C_3/C_9$ oligonucleotide; 1D proton spectra of the aromatic region of the oligonucleotides; 2D NOE of ^{Cl}C3/C9 oligonucleotide with H6−H1′ connectivity; temperature-dependent proton spectra in the imino region of the ^{Cl}C3/C9 oligonucleotide; magnetization-transfer experiment of the amino protons of the ^{Cl}C3/C9 oligo; nonlinear curve fitting from magnetization-transfer experiments of ^{Cl}C3/C9 oligo; and line widths of the amino protons of C3/C9, ^{m}C3/C9, and ^{Cl}C3/C9 oligonucleotides as a function of temperature. This material is available free of charge via the Internet at http://pubs.acs.org.

■ AUTHOR INFORMATION

Corresponding Author

*Phone:409-772-9678; E-mail: lasowers@utmb.edu.

Funding

This work was supported by grants CA50351 from the National Cancer Institute, GM083703 and GM066813 from the National Institute of General Medical Sciences, and the Welch Foundation (H-1592 and H-0037).

Notes

The authors declare no competing financial interest.

■ ACKNOWLEDGMENTS

We are grateful to the generous endowment from the Sealy and Smith Foundation to Sealy Center for Structural Biology at University of Texas Medical Branch. We thank Christie Shumate for crystallization of the DNA duplexes as well as the support of staff of SBC ID19 at APS, Argonne National Laboratory. The structure factors and coordinates of the ^{Cl}C and ^{m}C-containing dodecamers are deposited at the Protein Data Bank with accession numbers 4MGW and 4MKW, respectively. We thank Christopher Perry and Jonathan Neidigh (Loma Linda University) for help with quantum mechanical calculations and NMR experiments, respectively.

■ DEDICATION

This manuscript is dedicated to the fond memory of Victor Fung, Ph.D., a former Program Officer at NCI and former Scientific Review Officer of the Cancer Etiology study section of CSR, NIH, for his wisdom, compassion, integrity, love of sciences and the arts, incredible culinary skills, and, above all, contributions to the career development of so many investigators during his own distinguished career.

■ ABBREVIATIONS USED

^{m}C, 5-methylcystosine; ^{Cl}C, 5-chlorocytosine; ^{Br}C, 5-bromocytosine; HOCl, hypochlorous acid; T_m, melting temperature; MALDI-ToF-MS, matrix-assisted laser desorption/ionization time of flight mass spectrometry; GC/MS, gas chromatography−mass spectrometry; NOE, nuclear Overhauser effect

■ REFERENCES

(1) Sandoval, J., and Esteller, M. (2012) Cancer epigenomics: Beyond genomics. *Curr. Opin. Genet. Dev. 22*, 50−55.

(2) You, J. S., and Jones, P. A. (2012) Cancer genetics and epigenetics: Two sides of the same coin. *Cancer Cell 22*, 9−20.

(3) Shen, H., and Laird, P. W. (2013) Interplay between the cancer genome and epigenome. *Cell 153*, 38−55.

(4) Bird, A. P., and Wolffe, A. P. (1999) Methylation-induced repression—belts, braces, and chromatin. *Cell 99*, 451−454.

(5) Valinluck, V., Tsai, H. H., Rogstad, D. K., Burdzy, A., Bird, A., and Sowers, L. C. (2004) Oxidative damage to methyl-CpG sequences inhibits the binding of the methyl-CpG binding domain (MBD) of methyl-CpG binding protein 2 (MECP2). *Nucleic Acids Res. 32*, 4100−4108.

(6) Jones, P. A., and Baylin, S. B. (2007) The epigenomics of cancer. *Cell 128*, 683−692.

(7) McCabe, M. T., Brandes, J. C., and Vertino, P. M. (2009) Cancer DNA methylation: Molecular mechanisms and clinical implications. *Clin. Cancer Res. 15*, 3927−3937.

(8) Kanwal, R., and Gupta, S. (2012) Epigenetic modifications in cancer. *Clin. Genet. 81*, 303−311.

(9) Lewis, J. G., and Adams, D. O. (1987) Inflammation, oxidative DNA damage, and carcinogenesis. *Environ. Health Perspect. 76*, 19−27.

(10) Ames, B. N., Gold, L. S., and Willett, W. C. (1995) The causes and prevention of cancer. *Proc. Natl. Acad. Sci. U.S.A. 92*, 5258−5265.

(11) Lonkar, P., and Dedon, P. C. (2011) Reactive species and DNA damage in chronic inflammation: Reconciling chemical mechanisms and biological fates. *Int. J. Cancer 128*, 1999−2009.

(12) Whiteman, M., Jenner, A., and Halliwell, B. (1997) Hypochlorous acid-induced base modifications in isolated calf thymus DNA. *Chem. Res. Toxicol. 10*, 1240−1246.

(13) Winterbourn, C. C., and Kettle, A. J. (2000) Biomarkers of myeloperoxidase-derived hypochlorous acid. *Free Radical Biol. Med. 29*, 403−409.

(14) Badouard, C., Masuda, M., Nishino, H., Cadet, J., Favier, A., and Ravanat, J. L. (2005) Detection of chlorinated DNA and RNA nucleosides by HPLC coupled to tandem mass spectrometry as potential biomarkers of inflammation. *J. Chromatogr., B: Anal. Technol. Biomed. Life Sci. 827*, 26−31.

(15) Kang, J. I., and Sowers, L. C. (2008) Examination of hypochlorous acid-induced damage to cytosine residues in a CpG dinucleotide in DNA. *Chem. Res. Toxicol. 21*, 1211−1218.

(16) Mangerich, A., Knutson, C. G., Parry, N. M., Muthupalani, S., Ye, W., Prestwich, E., Cui, L., McFaline, J. L., Mobley, M., Ge, Z., Taghizadeh, K., Wishnok, J. S., Wogan, G. N., Fox, J. G., Tannenbaum, S. R., and Dedon, P. C. (2012) Infection-induced colitis in mice causes dynamic and tissue-specific changes in stress response and DNA damage leading to colon cancer. *Proc. Natl. Acad. Sci. U.S.A. 109*, 1820−1829.

(17) Seiberling, K. A., Chruch, C. A., Herring, J., and Sowers, L. C. (2012) Epigenetics of chronic rhinosinusitis and the role of the eosinophil. *Int. Forum Allergy Rhinol. 2*, 80−84.

(18) Valinluck, V., Liu, P., Kang, J. I., Jr., Burdzy, A., and Sowers, L. C. (2005) 5-Halogenated pyrimidine lesions within a CpG sequence context mimic 5-methylcytosine by enhancing the binding of the methyl-CpG-binding domain of methyl-CpG-binding protein 2 (MeCP2). *Nucleic Acids Res. 33*, 3057−3064.

(19) Lao, V. V., Darwanto, A., and Sowers, L. C. (2010) Impact of base analogues within a CpG dinucleotide on the binding of DNA by the methyl-binding domain of MeCP2 and methylation by DNMT1. *Biochemistry 49*, 10228−10236.

(20) Valinluck, V., and Sowers, L. C. (2007) Endogenous cytosine damage products alter the site selectivity of human DNA maintenance methyltransferase DNMT1. *Cancer Res. 67*, 946−950.

(21) Valinluck, V., and Sowers, L. C. (2007) Inflammation-mediated cytosine damage: A mechanistic link between inflammation and the epigenetic alterations in human cancers. *Cancer Res. 67*, 5583−5586.

(22) Lao, V. V., Herring, J. L., Kim, C. H., Darwanto, A., Soto, U., and Sowers, L. C. (2009) Incorporation of 5-chlorocytosine into

mammalian DNA results in heritable gene silencing and altered cytosine methylation patterns. *Carcinogenesis 30*, 886−893.
(23) Bennett, M. T., Rodgers, M. T., Hebert, A. S., Ruslander, L. E., Eisele, L., and Drohat, A. C. (2006) Specificity of human thymine DNA glycosylase depends on N-glycosidic bond stability. *J. Am .Chem. Soc. 128*, 12510−12519.
(24) Brennan, C. A., Van Cleve, M. D., and Gumport, R. I. (1986) The effects of base analogue substitutions on the cleavage by the EcoR1 restriction endonuclease of octadeoxyribonucleotides containing modified EcoR1 recognition sequences. *J. Biol. Chem. 261*, 7270−7278.
(25) Liu, P., Burdzy, A., and Sowers, L. C. (2002) Substrate recognition by a family of uracil-DNA glycosylases: UNG, MUG, and TDG. *Chem. Res. Toxicol. 15*, 1001−1009.
(26) Darwanto, A., Theruvathu, J. A., Sowers, J. L., Pascal, T., Goddard, W., 3rd, and Sowers, L. C. (2009) Mechanism of base selection by human single-stranded selective monofunctional uracil-DNA glycosylase. *J. Biol. Chem. 284*, 15835−15846.
(27) Fratini, A. V., Kopka, M. L., Drew, H. R., and Dickerson, R. E. (1982) Reversible bending and helix geometry in a B-DNA dodecamer: CGCGAATTBrCGCG. *J. Biol. Chem. 257*, 14686−14707.
(28) Kang, J. I., Jr., Burdzy, A., Liu, P., and Sowers, L. C. (2004) Synthesis and characterization of oligonucleotides containing 5-chlorocytosine. *Chem. Res. Toxicol. 17*, 1236−1244.
(29) Sowers, L. C. (2000) ^{15}N-Enriched 5-fluorocytosine as a probe for examining unusual DNA structures. *J. Biomol. Struct. Dyn. 17*, 713−723.
(30) Cui, Z., Theruvathu, J. A., Farrel, A., Burdzy, A., and Sowers, L. C. (2008) Characterization of synthetic oligonucleotides containing biologically important modified bases by matrix-assisted laser desorption/ionization time-of-flight mass spectrometry. *Anal. Biochem. 379*, 196−207.
(31) Theruvathu, J. A., Kim, C. H., Rogstad, D. K., Neidigh, J. W., and Sowers, L. C. (2009) Base pairing configuration and stability of an oligonucleotide duplex containing a 5-chlorouracil-adenine base pair. *Biochemistry 48*, 7539−7546.
(32) Theruvathu, J. A., Kim, C. H., Darwanto, A., Neidigh, J. W., and Sowers, L. C. (2009) pH-dependent configurations of a 5-chlorouracil-guanine base pair. *Biochemistry 48*, 11312−11318.
(33) Adams, P. D., Afonine, P. V., Bunkóczi, G. V., Chen, B., Davis, I. W., Echols, N., Headd, J. J., Hung, L.-W., Kapral, G. J., Grosse-Kunstleve, R. W., McCoy, A. J., Moriarty, N. W., Oeffner, R., Read, R. J., Richardson, D. D., Richardson, J. S., Terwilliger, T. C., and Zwart, P. H. (2010) PHENIX: A comprehensive Python-based system for macromolecular structure solution. *Acta Crystallogr. D66*, 213−221.
(34) Liu, M., Mao, X., Ye, C., Huang, H., Nicholson, J. K., and Lindon, J. C. (1998) Improved WATERGATE pulse sequences for solvent suppression in NMR spectroscopy. *J. Magn. Reson. 132*, 125−129.
(35) Hare, D. R., Wemmer, D. E., Chou, S. H., Drobny, G., and Reid, B. R. (1983) Assignment of the non-exchangeable proton resonances of d(C-G-C-G-A-A-T-T-C-G-C-G) using two-dimensional nuclear magnetic resonance methods. *J. Mol. Biol. 171*, 319−336.
(36) Weiss, M. A., Patel, D. J., Sauer, R. T., and Karplus, M. (1984) Two-dimensional ^{1}H NMR study of the lambda operator site OL1: A sequential assignment strategy and its application. *Proc. Natl. Acad. Sci. U.S.A. 81*, 130−134.
(37) Grzesiek, S., and Bax, A. (1993) The importance of not saturating water in protein NMR. Application to sensitivity enhancement and NOE measurements. *J. Am. Chem. Soc. 115*, 12593−12594.
(38) Michalczyk, R., and Russu, I. M. (1999) Rotational dynamics of adenine amino groups in a DNA double helix. *Biophys. J. 76*, 2679−2686.
(39) Jiang, L., and Russu, I. M. (2002) Internal dynamics in a DNA triple helix probed by (1)H-(15)N-NMR spectroscopy. *Biophys. J. 82*, 3181−3185.
(40) Moser, A., Guza, R., Tretyakova, N., and York, D. M. (2009) Density functional study of the influence of C5 cytosine substitution in base pairs with guanine. *Theor. Chem. Acc. 122*, 179−188.
(41) Frisch, M. J., Trucks, G. W., Schlegel, H. B., Scuseria, G. E., Robb, M. A., Cheeseman, J. R., Montgomery, J. A., Jr., Vreven, T., Kudin, K. N., Burant, J. C., Millam, J. M., Iyengar, S. S., Tomasi, J., Barone, V., Mennucci, B., Cossi, M., Scalmani, G., Rega, N., Petersson, G. A., Nakatsuji, H., Hada, M., Ehara, M., Toyota, K., Fukuda, R., Hasegawa, J., Ishida, M., Nakajima, T., Honda, Y., Kitao, O., Nakai, H., Klene, M., Li, X., Knox, J. E., Hratchian, H. P., Cross, J. B., Bakken, V., Adamo, C., Jaramillo, J., Gomperts, R., Stratmann, R. E., Yazyev, O., Austin, A. J., Cammi, R., Pomelli, C., Ochterski, J. W., Ayala, P. Y., Morokuma, K., Voth, G. A., Salvador, P., Dannenberg, J. J., Zakrzewski, V. G., Dapprich, S., Daniels, A. D., Strain, M. C., Farkas, O., Malick, D. K., Rabuck, A. D., Raghavachari, K., Foresman, J. B., Ortiz, J. V., Cui, Q., Baboul, A. G., Clifford, S., Cioslowski, J., Stefanov, B. B., Liu, G., Liashenko, A., Piskorz, P., Komaromi, I., Martin, R. L., Fox, D. J., Keith, T., Al-Laham, M. A., Peng, C. Y., Nanayakkara, A., Challacombe, M., Gill, P. M. W., Johnson, B., Chen, W., Wong, M. W., Gonzalez, C., and Pople, J. A. (2004) *Gaussian 03, revision A.1*, Gaussian, Inc., Wallingford, CT.
(42) Kupferschmitt, G., Schmidt, J., Schmidt, T., Fera, B., Buck, F., and Ruterjans, H. (1987) ^{15}N labeling of oligodeoxynucleotides for NMR studies of DNA-ligand interactions. *Nucleic Acids Res. 15*, 6225−6241.
(43) Ramesh, V., Xu, Y. Z., and Roberts, G. C. (1995) Site-specific ^{15}N-labelling of oligonucleotides for NMR: The trp operator and its interaction with the trp repressor. *FEBS Lett. 363*, 61−64.
(44) Acedo, M., Fabrega, C., Avino, A., Goodman, M., Fagan, P., Wemmer, D., and Eritja, R. (1994) A simple method for N-15 labeling of exocyclic amino groups in synthetic oligodeoxynucleotides. *Nucleic Acids Res. 22*, 2982−2989.
(45) SantaLucia, J., Jr., Allawi, H. T., and Seneviratne, P. A. (1996) Improved nearest-neighbor parameters for predicting DNA duplex stability. *Biochemistry 35*, 3555−3562.
(46) Lavery, R., Moakher, M., Maddocks, J. H., Petkeviciute, D., and Zakrzewska, K. (2009) Conformational analysis of nucleic acids revisited: Curves+. *Nucleic Acids Res. 37*, 5917−5929.
(47) Sowers, L. C., Shaw, B. R., and Sedwick, W. D. (1987) Base stacking and molecular polarizability: Effect of a methyl group in the 5-position of pyrimidines. *Biochem. Biophys. Res. Commun. 148*, 790−794.
(48) Lefebvre, A., Mauffret, O., el Antri, S., Monnot, M., Lescot, E., and Fermandjian, S. (1995) Sequence dependent effects of CpG cytosine methylation. A joint ^{1}H-NMR and ^{31}P-NMR study. *Eur. J. Biochem. 229*, 445−454.
(49) Fujii, S., Wang, A. H., van der Marel, G., van Boom, J. H., and Rich, A. (1982) Molecular structure of (m5 dC-dG)3: The role of the methyl group on 5-methyl cytosine in stabilizing Z-DNA. *Nucleic Acids Res. 10*, 7879−7892.
(50) Hansch, C., Leo, A., and Taft, R. W. (1991) A survey of Hammett substituent constants and resonance and field parameters. *Chem. Rev. 91*, 165−195.
(51) Petruska, J. P., Sowers, L. C., and Goodman, M. F. (1986) Comparison of nucleotide interactions in water, proteins and vacuum: Model for DNA polymerase fidelity. *Proc. Natl. Acad. Sci. U.S.A. 83*, 1559−1562.
(52) Zheng, H., Cai, Y., Ding, S., Tang, Y., Kropachev, K., Zhou, Y., Wang, L., Wang, S., Geacintov, N. E., Zhang, Y., and Broyde, S. (2010) Base flipping free energy profiles for damaged and undamaged DNA. *Chem. Res. Toxicol. 23*, 1868−1870.
(53) Balkwill, F., and Mantovani, A. (2001) Inflammation and cancer: Back to Virchow? *Lancet 357*, 539−545.
(54) Schmidt, A., and Weber, O. F. (2006) In memoriam of Rudolf Virchow: A historical retrospective including aspects of inflammation, infection and neoplasia. *Contrib. Microbiol. 13*, 1−15.